Journal of Applied Mechanics and Technical Physics, Vol. 47, No. 5, pp. 679–687, 2006

ON THE DISCHARGE CHARACTERISTIC AT THE DAM SITE AFTER DAM BREAK

V. I. Bukreev

UDC 532.532 + 532.59

A review of the information available in the literature is given, and new experimental data on the depth and discharge at the dam site after a total and a partial dam break are presented. It is shown that in the case of a partial dam break with the formation of a rectangular breach, the specific discharge per unit width of the breach is higher than the specific discharge in the case of a total dam break with the same excess initial energy in the headwater.

Key words: *dam break, discharge characteristic, even bottom, step, drop, sill, breach.*

Introduction. The solution of the hydrodynamic problem of dam break, which is of independent importance, can also be used to test methods for the calculation of catastrophic waves resulting, for example, from earthquakes, landslides, meteorite falls, strong explosions, shallow-water tsunami, quick stop of containers filled partially with a fluid, the striking of wind waves on a ship deck. At present, this problem has been solved using the model of potential fluid motion, in particular, the first approximation [1, 2] and higher approximation [3, 4] of shallow-water theory, Saint Venant equation [5, 6], the Euler and Navier–Stokes equations [7], and the equations taking into account turbulent mixing [8] and the interaction of water and air [7].

The dam break problem differs from the other problems of catastrophic waves in the clear formulation of the initial conditions. These conditions are only characterized by geometrical parameters L_i, the acceleration of gravity g, and the physical properties of water (in some models, in addition, by the properties of air). In the ideal fluid model, the physical properties of water are ignored. In this case, which is degenerate from the viewpoint of dimension theory, the system has freedom in choosing the characteristic velocity. In other words, the characteristic Froude number in this formulation of the problem is uniquely determined by geometrical parameters. This simplifies not only the calculations but also physical modeling because experiments can be performed on fairly small setups. In the ideal fluid model, it suffices to observe geometrical similarity in order for the Froude number to be the same as under natural conditions. In a viscous fluid, the Froude number also depends on the Reynolds number. However, even for a small (about 10-cm) initial free-surface level difference, the Reynolds number $\mathrm{Re} > 10^4$ and the flow at the dam site virtually does not depend on this parameter. For large initial differences between the headwater and tailwater levels, the water continuity may be interrupted, in which case the results of the classical theory and laboratory experiments, strictly speaking, are not applicable. This process, however, has a local nature. At fairly large distances from the dam site, its influence is manifested mainly in the fact that the initial potential energy stored in the dam is not entirely converted to the energy of wave motion. Quantitative information on such local energy losses is currently not available.

Calculations of dam-break waves at large distances and times for conditions of extremely complex geometry and hydraulics resistance of real riverbeds have been performed on the basis of the Saint Venant equations [5, 6, 9, 10], which use the assumption of hydrostatic pressure distribution and empirical information on hydraulic resistances. In calculations for more complex models, a rectangular channel with an even horizontal bottom is usually considered. Only recently has the dam break problem been solved in the first shallow-water approximation

Lavrent'ev Institute of Hydrodynamics, Siberian Division, Russian Academy of Sciences, Novosibirsk 630090; bukreev@hydro.nsc.ru. Translated from Prikladnaya Mekhanika i Tekhnicheskaya Fizika, Vol. 47, No. 5, pp. 77–87, September–October, 2006. Original article submitted September 6, 2005; revision submitted October 21, 2005.

for an infinitely wide channel with a drop (a sharp downstream lowering of the bottom) and a step (a sharp downstream elevation of the bottom) [2, 11, 12].

The calculations are significantly simplified by specifying the conjugation conditions at the dam site in the form of the so-called discharge characteristic $Q(h)$ [13], where Q is the volumetric discharge and h is the depth. This allows downstream processes of greatest practical interest to be considered separately from upstream processes. The present paper gives literature data and additional information on this discharge characteristic.

Generally, the hydrodynamic processes due to dam break depend on time even in an infinitely long channel since new portions of quiescent fluid are constantly set in motion. However, at the dam site, the discharge characteristic rapidly becomes unchanged and the flow becomes stationary. In calculations, it is usually assumed that the stationary flow regime at the dam site is established instantaneously. In practice, the rate of attainment of the stationary regime is determined by the inertia of hydrodynamic processes and the nature of dam break. The initial stage of the hydrodynamic processes resulting from a total dam break in a rectangular channel with an even horizontal bottom has been investigated on the basis of numerical calculations using five mathematical models (including models with the Euler and Navier–Stokes equations [7]) and experimentally (see [14]).

In the case of a partial dam break, information on the stationary flow over obstacles of various shapes in an open channel is useful. In this case, it is necessary to take into account that in the dam break problem, only part of the excess potential energy specified in the form of an initial free-surface level difference passes downstream. The other part of it is spent by the level-fall wave in the headwater to cause the quiescent fluid to move. The discharge characteristic determines, in particular, the ratio of these parts.

Open-channel flows are classified using the notions of the critical depth h_* and the critical velocity V_* [13]:

$$h_* = (q^2/g)^{1/3}, \qquad V_* = q/h_*, \qquad q = Q/B$$

(B is the width of the rectangular channel and q is the specific discharge); a more detailed classification uses the notions of the second critical depth $h_{**} \approx 0.77h_*$, its related second critical velocity $V_{**} = q/h_{**}$ [15], and the so-called jump functions P [13]:

$$P = Q^2/(gS) + z_c S$$

(S is the area of the flow cross section considered and z_c is the vertical coordinate of the center of gravity of this cross section relative to the channel bottom). In the first shallow-water approximation, the value of P is retained under transition from supercritical to subcritical flow in a classical hydraulic jump. For a rectangular channel and normalization using B and h_*, we have

$$P^0 = \frac{P}{Bh_*^2} = \frac{h_*}{h} + \frac{1}{2}\Big(\frac{h}{h_*}\Big)^2. \tag{1}$$

Here $h > 0$ is the flow depth in the cross section considered; two values of h/h_* correspond to one value of P^0.

The wave patterns after dam break differ significantly for the free and submerged regimes of head- and tail-water conjugation. (The conjugation regime is called submerged if downstream processes do not influence upstream processes [13].) The cases of the initially dry and flooded bottom in the tailwater [1] are also different.

Information Known from Experiments Performed Previously. Laboratory experiments [16, 17] have shown that in the case of a total dam break in a rectangular channel with an even horizontal bottom for the free regime of head and tail conjugation, the values of h_0, q_0, and P^0 and the fluid velocities u_0 at the dam site are fairly well predicted by the first shallow-water approximation [1]:

$$h_0 = h_* = 4h_-/9, \qquad q_0 = 8g^{1/2}h_-^{3/2}/27, \qquad P^0 = 1.5, \qquad u_0 = V_* = (gh_0)^{1/2}, \tag{2}$$

where h_- is the initial headwater depth. The theoretical estimate for the region of existence of the free regime [1]

$$0 \leqslant h_+ < 0.138h_-$$

(h_+ is the initial tail-water depth) is also supported by experimental data [16, 17].

In the case of one-dimensional stationary flow and a hydrostatic pressure distribution, the specific energy of the cross section can be determined from the expression

$$E = h + u^2/(2g),$$

where h is the depth and u is the speed. For the free regime at the dam site, $E_0 = 2h_-/3$. This implies that in the case of an initially dry bottom ($h_+ = 0$), 2/3 of the initial energy passes downstream, and 1/3 of it is carried away by the level-fall wave upstream.

For the submerged regime ($0.138 < h_+/h_- \leqslant 1$), the values of h_0 and q_0 depend on the ratio h_-/h_+. In the first shallow-water approximation, they are found from a system of algebraic equations [1]. Experiments [17] have shown that for the submerged regime, the theory overestimates the value of h_0. The largest deviation from the experimental value is observed in the vicinity of the value $h_+/h_- = 0.3$ but it does not exceed 10%. The theory in question underestimates the wave propagation speed in the headwater by approximately 30% compared to its experimental value and inadequately describes the wave in the tailwater in the case of an initially dry bottom [17].

If an initial level difference occurs immediately above a bottom drop, then, for the free regime, the first shallow-water approximation [2] predicts instantaneous establishment of critical flow in this cross section with the parameters defined by formulas (2), in which h_- is measured from the bottom upstream of the drop. In this case, the free regime exists in the range $0 \leqslant h_+ < \delta + h_*$ (δ is the height of the drop and h_+ is measured from the bottom downstream of the drop).

Experiments [18] have shown that for the free regime, the second critical depth h_{**} is established immediately above the drop. However, at a distance of order h_- upstream, the critical depth h_* is also established in experiments, so that the indicated deviation from the theory virtually does not influence the wave pattern in the tailwater. The theory overestimates the dimensions of the region of existence of the free regime by 16% and underestimates the value of h_0 in the submerged regime by 10–25%. As in the case of an even bottom, the theory in question underestimates the propagation speed of the fall-level wave in the tailwater and does not describe undulations (the fluctuations of the free-surface level behind the leading front of the hydraulic jump).

In the first shallow-water approximation, the discharge characteristic can also be calculated in the case of an initial level difference above a bottom step. The calculations reduce to solving a system of algebraic equations [11]. In the theory, a jump of the free-surface level occurs immediately above the step. In experiments, such a jump is absent [11]. However, the experimental value of h_0 at the dam site agrees well with the height of the middle of the theoretical jump. A comparison of the theory and experiments for other flow characteristics [11] yields qualitatively the same results as in the cases of an even bottom and a drop.

In practice, a total dam break is improbable. Therefore, the formulations of the problems examined above lead, as a rule, to a significant overestimation of the mass, momentum, and energy that pass to the tailwater. The next step toward more adequate modeling of the real situation is to study the discharge characteristic in the case of an initial free-surface level difference above a sill (a combination of a step and a drop) that extends over the entire width of the channel. This case was experimentally investigated in [19] for identical bed levels before and after the sill. In comparison with the case of a total dam break, this formulation of the problem contains two more geometrical parameters: the height δ and the length l of the sill. In the experiments of [19], the following parameter ranges were examined: $h_+^0 < \delta^0$ (the free regime), $3 \cdot 10^4 < g^{1/2}H^{3/2}/\nu < 1.8 \cdot 10^5$, $0.15 < \delta^0 < 1.4$, and $0.1 < l^0 < 1.5$ (ν is the kinematic viscosity of water; the superscript 0 indicates that the corresponding quantity is normalized by the head above the sill crest $H = h_- - \delta$). The experiments showed that for values $\delta^0 > 0.4$ over the entire examined range of l^0, the critical depth $h_* = 4H/9$ was established above the sill in a certain flow cross section. The second critical depth h_{**} was established immediately above the back face of the sill. It should be noted that for stationary flow with a specified discharge over a fairly high sill of length $2 < l^0 < 12$, the critical depth was also established above the sill in a certain cross section [13], and the second critical depth was established above the back face of the sill [20].

Thus, in the case of a fairly high and not too long sill that extends over the entire width of the channel, the discharge characteristic is defined by formulas (2) in which h_- needs to be replaced by the head pressure above the sill crest H. The next step to the adequate determination of the discharge characteristic for a partial dam break is to study the processes at an outlet whose width is smaller than the channel width.

Experiments with a Breach of Limited Width. An obstacle, shown schematically in Fig. 1, was placed in a rectangular channel of width $2B = 20.2$ cm and length 7.2 m with a horizontal bottom. On the right, the channel ended with a vertical wall. The front face of the obstacle was at a distance of 4.46 m upstream of this wall. The left open end of the channel was connected to a tank 1 m wide and was at a distance of 1.32 m from the end wall of the tank. The obstacle simulated half of a symmetric rectangular breach of width $2b$ and length l with

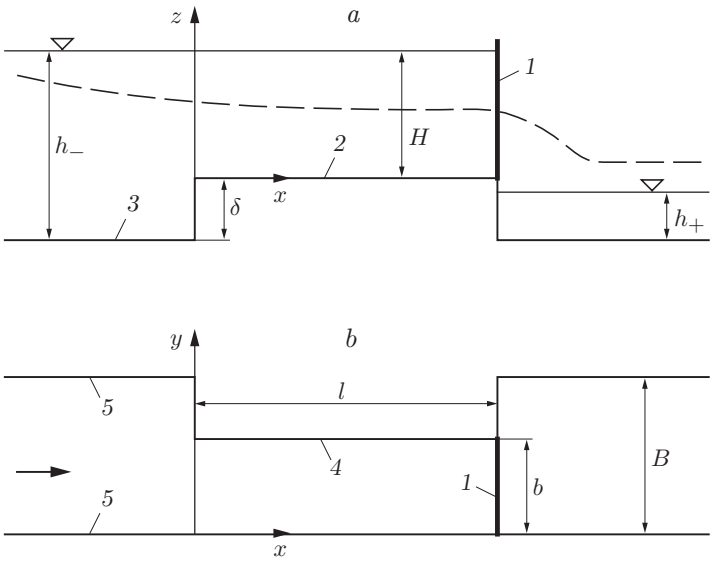

Fig. 1. Diagram of the breach: (a) side view; (b) top view; 1) shield; 2) breach crest; 3) channel bottom; 4) side face of the breach; 5) channel sidewalls; the free-surface water level after the removal of the shield is shown by a dashed curve.

sharp edges at the entrance and exit. The results below are given for one combination of parameters: $l = 69$ cm, $b = 10$ cm, and $\delta = 5.5$ cm. However, for the normalization by H and in view of the indicated feature of the problem, from the standpoint of the theory of dimension, these results can be extrapolated to a fairly wide range of geometrical parameters of the problem and characteristic values of the Froude number.

The initial free-surface level difference was produced by a flat shield placed immediately behind the obstacle. Next, we consider only the case $h_+ < \delta$, where the head and tail conjugation regime behind the obstacle is free. At the time $t = 0$, the shield was lifted upward by means of a lever. The time the lower edge of the shield emerged from water did not exceed 0.05 sec. The processes in the vicinity of the breach were recorded by a video camera. The velocities of water motion in the breach were studied by means of the particle image velocimetry (PIV) technique (using technical devices and computer programs from Dantec Dynamics).

Figure 2 gives flow patterns in the breach at various times $t^0 = t(g/H)^{1/2}$, where H is the initial head above the crest of the breach. (The vertical scale in Fig. 2 is 1.2 times larger than the horizontal scale.) As in the case of removal of a shield in a channel without an obstacle [14], a characteristic angular point is first formed on the free surface; downstream of this point, the free-surface profile is concave, and upstream of it, the profile is convex (Fig. 2a). Then, the free surface in the breach becomes smooth for a time (Fig. 2b). At $t_1^0 > 15$, the flow is separated from the front side edge of the breach and quasistationary oblique waves are formed (Fig. 2c). The term quasistationary means that oblique waves are characterized by fluctuations in space and time. As a result of the separation, the flow has a three-dimensional nature and the pressure distribution with depth differs from the distribution corresponding to the hydrostatic law. The assumption of a hydrostatic pressure distribution is one of the basic assumptions in the first shallow-water approximation. Therefore, for the flow considered, this theory, strictly speaking, is not applicable. Figure 2d shows the wave reflected from the closed right wall of the channel.

Figure 3 shows four points on the transparent sidewall of the channel, for which the vertical coordinates of the free surface relative to the bottom of the breach h_i $(i = 1, 2, 3, 4)$ were determined by computer processing of video records. The longitudinal coordinates of these points are denoted by x_i. The solid curve corresponds to the position of the free surface on the front wall of the channel, and the dashed curve to the position of the free surface on the side face of the breach (see Fig. 2c). The analysis was performed for the flow cross sections with the coordinates $x_1^0 = 0$, $x_2^0 = 1.41$, $x_3^0 = 3.93$, and $x_4^0 = l^0 = 4.76$ (the coordinates are normalized by $H = 14.5$ cm). In these cross sections, the depth variation along the coordinate y^0 was insignificant (see Fig. 2).

Figure 4 gives experimental curves of $h_i^0(t^0)$, where $h_i^0 = h_i/H$. The dashed line corresponds to the experimental value $h_* = (q^2/g)^{1/3}$ normalized by H. Information on the experimental value of q is given below. In Fig. 4,

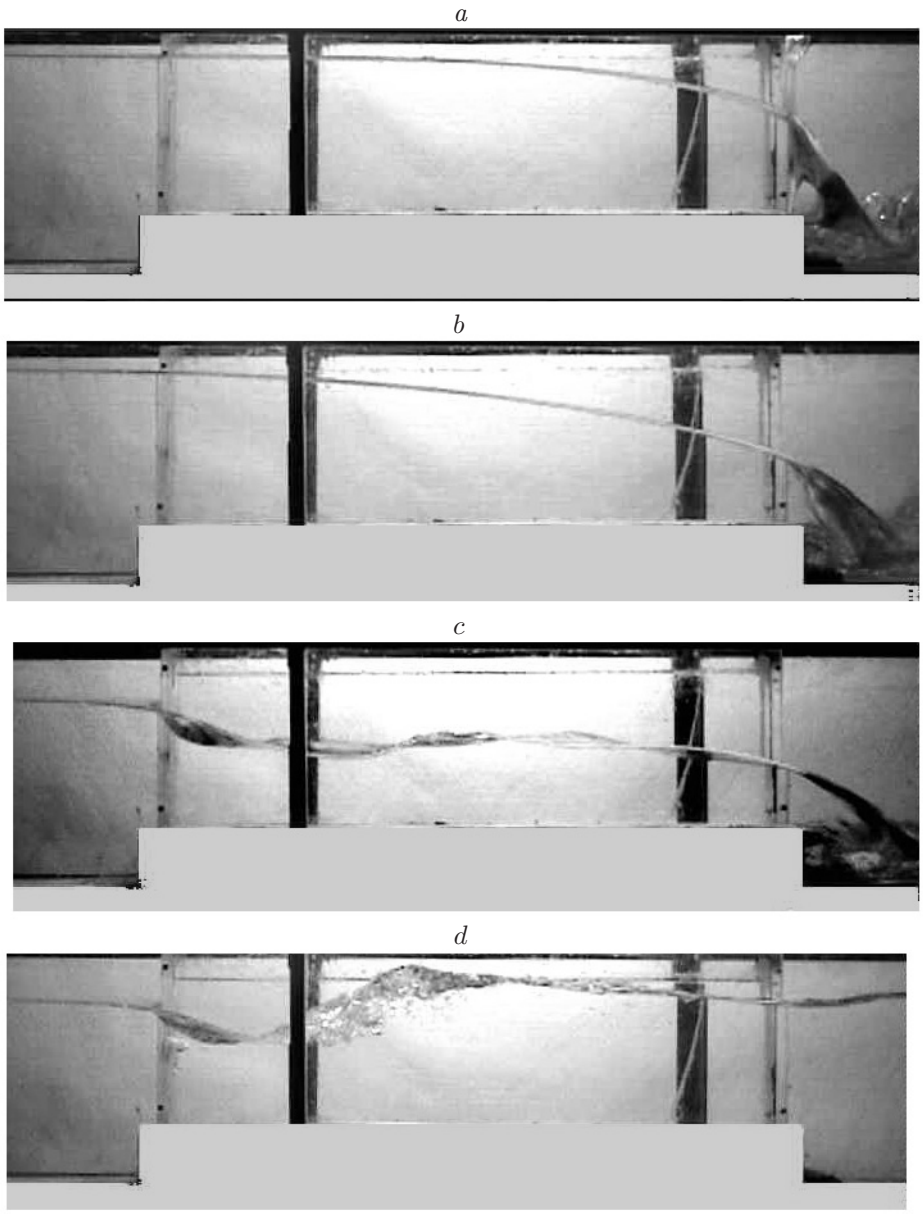

Fig. 2. Flow pattern in the breach at times $t^0 = 5.2$ (a), 9.7 (b), 30.7 (c), and 135 (d); $H = 14.5$ cm.

it is evident that the functions h_i^0 rapidly reach constant values. This necessarily indicates that the flow regime in the breach becomes quasistationary. In cross sections 1 and 3, the time intervals in which the transition processes occur are approximately identical: $t_1^0 \approx t_3^0 \approx 20$. For cross section 2, $t_2^0 \approx 27$. The constant depth above the back face of the breach (cross section 4) is established the most rapidly (in $t_4^0 \approx 13$).

The constant values h_2^0, h_3^0, and h_4^0 differ insignificantly from the values of the corresponding quantities for a sill that extends over the entire width of the channel [19]. However, all these values are smaller than the experimental critical depth h_*^0. In the case of a hydrostatic pressure distributions, this implies that the flow is supercritical.

In a channel of finite length, the time of existence of the stationary regime is limited because of the superposition of the direct and reflected waves. The deviation of the depth from the stationary value indicates that the reflected wave has arrived at the flow cross section considered. For the curves in Fig. 4, the first increase in the

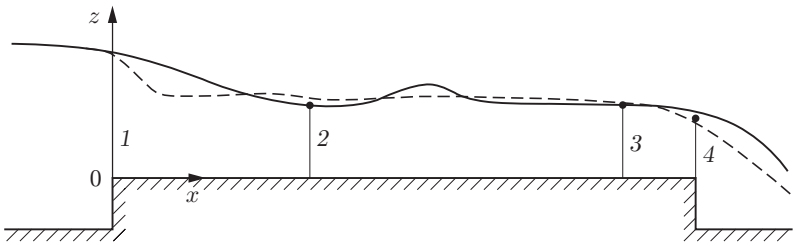

Fig. 3. Flow cross sections chosen for depth measurements: $x^0 = 0$ (1), 1.41 (2), 3.93 (3), and 4.76 (4); the solid curve shows the position of the free surface on the front wall of the channel and the dashed curve is the same on the side face of the breach.

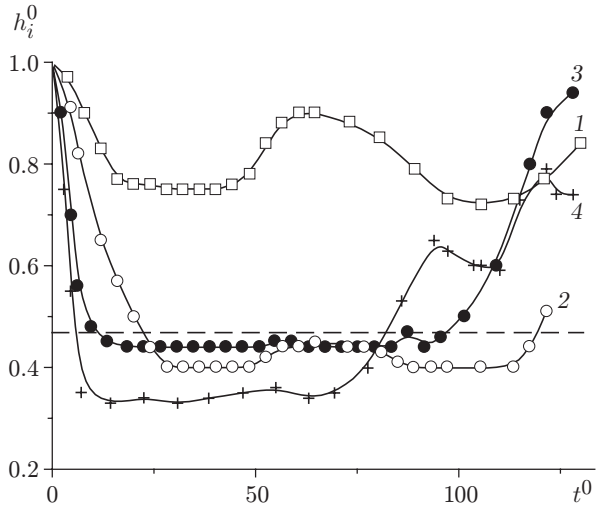

Fig. 4. Depth variation with time: curves 1–4 refer to the flow cross sections in Fig. 3; the dashed line refers to the experimental critical depth.

depth at $t^0 \approx 45$ is related to the arrival of the reflected wave from the headwater. The response to this reflected wave begins with a very small shift in time from cross section to cross section from upstream to downstream; the increase in depths in sections 2–4 is insignificant. This is due to the fact that the arrival of the examined reflected wave leads to an increase in the potential energy, and, hence, to a decrease in the kinetic energy at the entrance to the breach.

The next increase in depth in the examined cross sections is related to the arrival of the reflected wave from the tailwater. This wave propagates over the supercritical reverse flow; therefore, the response to it begins with an appreciable shift in time from cross section to cross section from downstream to upstream. The depth behind this wave reaches the value $0.93H$ (see Fig. 2d), so that a significant part of the kinetic energy is again converted to potential energy.

Figure 5a–c gives stationary profiles of the longitudinal velocity component u^0 and vertical velocity component w^0 in cross sections 2–4, respectively. [The velocities were obtained by the PIV technique and normalized by $(gH)^{1/2}$.] Measurements for various values of the coordinate y^0 showed that in the indicated cross sections, the flow nonuniformity along this coordinate did not exceed 5%. The quantitative data in Fig. 5 and in Table 1 were obtained for $H = 16$ cm and $y^0 = 0.125$.

Table 1 lists the following flow characteristics (the angular brackets denote averaging over the depth): $\langle u^0 \rangle = \langle u \rangle / (gH)^{1/2}$, $\langle w^0 \rangle = \langle w \rangle / (gH)^{1/2}$, $q^0 = \langle u^0 \rangle h^0$, $h_*^0 = (q^0)^{2/3}$, $\mathrm{Fr} = \langle u^0 \rangle^2 / h^0 = (h_*^0/h^0)^3$, and $E^0 = h^0 + (\langle u^0 \rangle^2 + \langle w^0 \rangle^2)/2$; the value of P^0 was calculated by formula (1). The bottom row of Table 1 gives the corresponding values for the case of a total dam break.

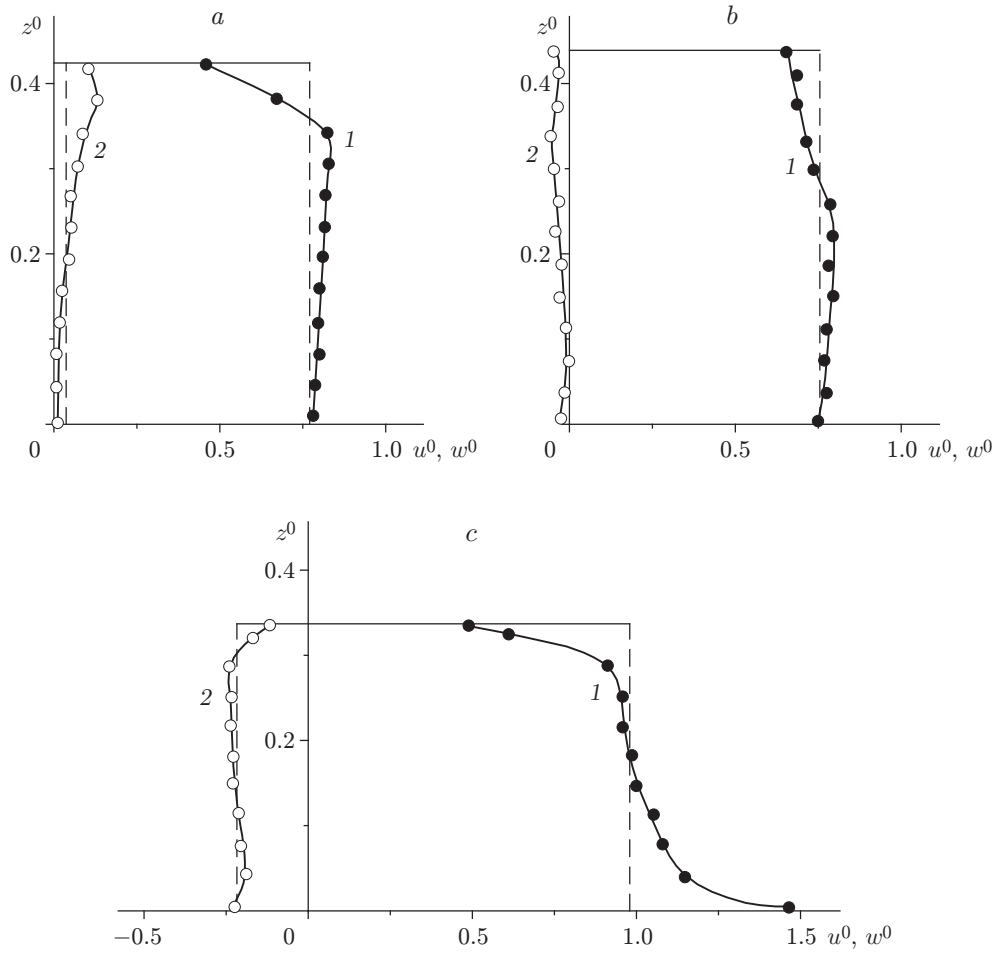

Fig. 5. Profiles of the longitudinal velocity component u^0 (curve 1) and vertical velocity component w^0 (curve 2) in cross sections 2 (a), 3 (b), and 4 (c).

TABLE 1

Cross section number in Fig. 3	x^0	h^0	$\langle u^0 \rangle$	$\langle w^0 \rangle$	q^0	h_*^0	Fr	P^0	E^0
2	1.41	0.425	0.765	0.044	0.325	0.473	1.377	1.517	0.719
3	3.93	0.441	0.735	−0.027	0.324	0.473	1.225	1.507	0.711
4	4.76	0.333	0.980	−0.208	0.326	0.474	2.884	1.670	0.835
Case $b/B = 1$, $\delta = 0$, $h_+^0 = 0$	0	4/9	2/3	0	8/27	4/9	1	3/2	2/3

The data presented in Table 1 allow the following conclusions to be to drawn. The specific discharge per unit width of the breach is retained in all three cross sections, as should be the case in the stationary regime. At the same time, this discharge is larger than the specific discharge per unit width of the channel in the case of a total dam break (see the bottom row of Table 1). This is due to the fact that the fluid enters the breach not only along the axis x but also sideways. It should be taken into account that in calculation of the total discharge Q in dimensional form, the specific discharge values given in the table need to be multiplied by $2bg^{1/2}(h_- - \delta)^{3/2}$ in the case of a symmetric breach and by $2Bg^{1/2}h_-^{3/2}$ in the case of a total dam break.

The values of h^0 are smaller and the values of the Froude number (Fr) and P^0 are larger than the corresponding critical values, so that in the cross sections discussed here, the flow is supercritical. In cross section 4, the

vertical velocity component is about 21% of the longitudinal components; therefore, at the exit from the breach, the deviations from the hydrostatic pressure distribution are rather considerable. In cross section 2, the vertical component is 5.8% of the longitudinal components, and in cross section 3, it is only 3.7%. The quantity P^0 varies along the flow, which is a consequence of both the deviations from the hydrostatic pressure distribution and the fact that for small values of l^0, a developed hydraulic jump is not formed in the breach (see Fig. 2).

In cross sections 2 and 3, the values of E^0 are approximately identical, as should be the case according to the hydrostatic pressure distribution, and on the average, they are 71.5% of the value of H. From this estimate of E^0, it follows that in the free regime, the level-fall wave in the headwater carries away 28.5% of the excess initial potential energy, which is 7% smaller than that in the case of a total dam break.

For cross section 4, the adopted estimation algorithm obviously gives an overestimated value of E^0 due to of a significant deviation from the hydrostatic pressure distribution. Water in the form of a concentrated jet flows from the breach to the tailwater, and the average pressure in the exit section of the breach is below atmospheric pressure. In the free regime, air (see Fig. 2b and c) can be entrained under the jet. At a distance downstream from the breach, the tailwater depth the varies significantly on the transverse coordinate y. In the free regime, the free-surface level near the channel wall is lower than that on the jet axis.

Using the average value E^0 in cross sections 2 and 3, in which the pressure distribution differs insignificantly from the hydrostatic distribution, it is possible to estimate the discharge coefficient of the breach m. From the definition of m [13] and the physical meaning of E^0, it follows that

$$m = \frac{q}{(2g)^{1/2}(E^0 H)^{3/2}}, \qquad q = \frac{q^0}{g^{1/2}H^{3/2}}.$$

Then,

$$m = \frac{q^0}{\sqrt{2}\,E^0}.$$

According to the data given in Table 1, $m = 0.38$. According to the reference data [13], for stationary flow over a sill extending over the entire width of the channel, $m = 0.30$–0.38, the smaller value corresponds to a sharp-edged sill, and the larger value to a sill with a rounded edge. The fact that the discharge coefficient of a sharp-edged breach is on the upper bound of the indicated range is due to flow separation from the front side edge with the subsequent attachment to the side face breach. An increase in the discharge coefficient is due to a pressure decrease in the separation zone, which is accompanied by additional entrainment of the fluid in the breach. An example of a similar effect in hydraulics is a considerable increase in the discharge for fluid flow through a Borda cylindrical nozzle compared to flow from an orifice in a thin wall.

The author expresses gratitude to E. V. Ermanyuk and V. A. Kostomakha for PIV velocity measurements.

This work was supported by the Russian Foundation for Basic Research (Grant No. 04-01-00040) and the Integration Program No. 3.13.1 of the Russian Academy of Sciences and the Siberian Division of the Russian Academy of Sciences.

REFERENCES

1. J. J. Stoker, *Water Waves*, Interscience, New York (1957).
2. V. V. Ostapenko, "Dam break flows over a bottom step," *J. Appl. Mech. Tech. Phys.*, **44**, No. 6, 495–505 (2003).
3. V. Yu Liapidevskii, "Shallow-water equations with dispersion. Hyperbolic model," *J. Appl. Mech. Tech. Phys.*, **39**, No. 2, 194–199 (1998).
4. V. B. Barakhnin, T. V. Krasnoshchekova, and I. N. Potapov, "Reflection of a dam-break wave at a vertical wall. Numerical modeling and experiment," *J. Appl. Mech. Tech. Phys.*, **42**, No. 2, 269–275 (2001).
5. A. A. Atavin, O. F. Vasil'ev, A. F. Voevodin, and S. M. Shugrin, "Numerical methods for the solution of one-dimensional problems of hydraulics," *Vodn. Resursy*, **4**, 38–47 (1983).
6. V. V. Belikov, A. A. Zaitsev, and A. N. Militeev, "Mathematical modeling of complex segments of large river-beds," *Vodn. Resursy*, **29**, No. 6, 698–705 (2002).

7. G. Colicchio, A. Colagrossi, M. Greco, and M. Landrini, "Free-surface flow after a dam break: A comparative study," *Schiffstechnik*, **49**, No. 3, 95–104 (2002).
8. V. Yu. Liapidevskii, "Structure of a turbulent bore in a homogeneous fluid," *J. Appl. Mech. Tech. Phys.*, **40**, No. 2, 238–248 (1999).
9. O. F. Vasil'ev "Mathematical modeling of hydraulic and hydrological processes in water reservoirs and water courses: Review of the research performed at the Siberian Division of the Russian Academy of Sciences," *Vodn. Resursy*, **26**, No. 5, 600–611 (1999).
10. V. V. Belikov and A. N. Militeev, "Two-layer mathematical model of catastrophic high waters," *Vychisl. Tekhnol.*, **1**, No. 3, 167–174 (1992).
11. V. I. Bukreev, A. V. Gusev, and V. V. Ostapenko, "Open-channel waves that form after removal of a shield ahead of an uneven shelf-type bottom," *Vodn. Resursy*, **31**, No. 5, 540–545 (2004).
12. V. I. Bukreev, A. V. Gusev, and V. V. Ostapenko, "Free-surface discontinuity decay above a drop of a channel bottom," *Izv. Ross. Akad. Nauk, Mekh. Zhidk. Gaza*, **6**, 72–83 (2003).
13. P. G. Kiselev, *Handbook on Hydraulic Calculations* [in Russian], Gosénergoizdat, Moscow (1957).
14. V. I. Bukreev and A. V. Gusev, "Initial stage of generation of dam-break waves," *Dokl. Ross. Akad. Nauk*, **401**, No. 5, 619–622 (2005).
15. V. I. Bukreev, "On the critical velocities and depths for nonuniform stationary flow in an open channel," *Vodn. Resursy*, **31**, No. 1, 40–45 (2004).
16. R. F. Dressler, "Comparison of theories and experiments for the hydraulic dam-break wave," it Int. Assoc. Sci. Hydrol., **3**, No. 38, 319–328 (1954).
17. V. I. Bukreev, A. V. Gusev, A. A. Malysheva, and I. A. Malysheva, "Experimental verification of the gas-hydraulic analogy by the example of the dam break problem," *Izv. Ross. Akad. Nauk, Mekh. Zhidk. Gaza*, **5**, 143–152 (2004).
18. V. I. Bukreev and A. V. Gusev, "Gravity waves due to discontinuity decay over an open-channel bottom drop," *J. Appl. Mech. Tech. Phys.*, **44**, No. 4, 506–515 (2003).
19. V. I. Bukreev, "On the water depth in the breach during a partial dam break," *Izv. Ross. Akad. Nauk, Mekh. Zhidk. Gaza*, **5**, 115–123 (2005).
20. V. I. Bukreev, "Undular jump in open-channel flow over a sill," *Appl. Mech. Tech. Phys.*, **42**, No. 4, 596–602 (2001).